

## Identification of Active Sites in Gold-Catalyzed Hydrogenation of Acrolein

Christian Mohr, Herbert Hofmeister,<sup>\*,†</sup> Jörg Radnik,<sup>‡</sup> and Peter Claus

Contribution from the Department of Chemistry, Institute of Chemical Technology II, Darmstadt University of Technology, Petersenstrasse 20, D-64287 Darmstadt, Germany, Max-Planck-Institute of Microstructure Physics, Weinberg 2, D-06120 Halle, Germany, and Institute for Applied Chemistry Berlin-Adlershof e.V., Rudower Chaussee 5, D-12489 Berlin, Germany

Received June 17, 2002; E-mail: hof@mpi-halle.mpg.de

**Abstract:** The active sites of supported gold catalysts, favoring the adsorption of C=O groups of acrolein and subsequent reaction to allyl alcohol, have been identified as edges of gold nanoparticles. After our recent finding that this reaction preferentially occurs on single crystalline particles rather than multiply twinned ones, this paper reports on a new approach to distinguish different features of the gold particle morphology. Elucidation of the active site issue cannot be simply done by varying the size of gold particles, since the effects of faceting and multiply twinned particles may interfere. Therefore, modification of the gold particle surface by indium has been used to vary the active site characteristics of a suitable catalyst, and a selective decoration of gold particle faces has been observed, leaving edges free. This is in contradiction to theoretical predictions, suggesting a preferred occupation of the low-coordinated edges of the gold particles. On the bimetallic catalyst, the desired allyl alcohol is the main product (selectivity 63%; temperature 593 K, total pressure  $p_{\text{total}} = 2$  MPa). From the experimentally proven correlation between surface structure and catalytic behavior, the edges of single crystalline gold particles have been identified as active sites for the preferred C=O hydrogenation.

### Introduction

The selective hydrogenation of  $\alpha,\beta$ -unsaturated aldehydes to the corresponding unsaturated alcohols is not only of commercial relevance in fine chemical and pharmaceutical intermediate production<sup>2</sup> but also of specific scientific interest.<sup>3</sup> Thermodynamics favors hydrogenation of the C=C over the C=O group (stronger negative free reaction enthalpy of 35 kJ mol<sup>-1</sup>). Besides, for kinetic reasons, the C=C bond is more reactive than the bond of C=O group. Nevertheless, it is challenging to design catalysts enabling the preferred hydrogenation of the C=O group versus C=C.

Differences in activity on different metals are mainly due to different extensions of their d orbitals.<sup>4</sup> However, it is more complicated to control the intramolecular selectivity being more important for this type of reaction, since it is influenced by various factors.<sup>4,5</sup> Structure sensitivity is reported by many authors;<sup>4-7</sup> that is, the reactivity (activity and/or selectivity)

depends on the metal particle size. Often the selectivity to the desired unsaturated alcohol increases with increasing particle size in a certain size range, even though some measurements seem to be contradictory.<sup>4,5</sup> Thus, it seems to be clear that the reactants exhibit different adsorption behavior on different surface sites (i.e., active sites) of the active metal component, leading to different yields of the desired unsaturated alcohol.<sup>3</sup> An explanation should also consider that for this reaction active sites may include certain ensembles or groups of atoms.<sup>8</sup>

Among the previously mentioned reactions, the hydrogenation of acrolein to allyl alcohol is considered most difficult to be realized because of the lack of space-filling substituents at the C=C group. Hence, the selectivity to allyl alcohol on conventional hydrogenation catalysts is generally low.<sup>9</sup> Better results are achieved using silver<sup>10</sup> or gold particles on oxide supports.<sup>11,12</sup>

During the past few years, gold has attracted growing interest in catalyst research, since it has been shown, namely by Haruta and co-workers,<sup>13</sup> that gold nanoparticles with sizes below 5

<sup>†</sup> Max-Planck-Institute of Microstructure Physics.

<sup>‡</sup> Institute for Applied Chemistry Berlin-Adlershof e.V.

- (1) Mohr, C.; Hofmeister, H.; Claus, P. *J. Catal.*, accepted for publication.
- (2) (a) Augustine, R. L. *Heterogeneous Catalysts in Organic Synthesis*, Dekker: New York, 1995. (b) Bauer, K.; Garbe, D. In *Ullmann's Encyclopedia of Industrial Chemistry*, 6th ed.; (Electronic Release) 2000.
- (3) Claus, P. *Topics in Catalysis*; Special Issue *Fine Chemicals Catalysis, Part II*; Somorjai, G. A., Thomas, J. M., Blackmond, D., Leitner, W., Eds.; Baltzer Science Publishers: Bussum, The Netherlands, 1998; Vol 5, pp 51-62.
- (4) Gallezot, P.; Richard, D. *Catal. Rev.—Sci. Eng.* **1998**, *40*, 81-126.
- (5) Coq, B.; Figueras, F. *Coord. Chem. Rev.* **1991**, *178-180*, 1753-1783.
- (6) Claus, P.; Hofmeister, H. *J. Phys. Chem. B* **1999**, *103* (14), 2766-2775.
- (7) Englisch, M.; Jentys, A.; Lercher, J. A. *J. Catal.* **1997**, *166* (1), 25-35.

- (8) Che, M.; Bennett, C. O. *Adv. Catal.* **1989**, *36*, 55-172.
- (9) (a) Ponec, V. *Appl. Catal. A* **1997**, *149*, 27-48. (b) Marinelli, T. B. L. W.; Ponec, V. *J. Catal.* **1995**, *156*, 51-59. (c) Marinelli, T. B. L. W.; Naarburs, S.; Ponec, V. *J. Catal.* **1995**, *151*, 431-438.
- (10) Claus, P.; Lucas, M. *EuropaCat V*, Sept 2nd-7th, 2001; Limerick, Abstracts book IV, Sympos. 19, *Catalysis by Silver and Gold*, 19-P-15.
- (11) Claus, P.; Brueckner, A.; Mohr, C.; Hofmeister, H. *J. Am. Chem. Soc.* **2000**, *122* (46), 11430-11439.
- (12) Schimpf, S.; Lucas, M.; Mohr, C.; Rodemerk, U.; Brückner, A.; Radnik, J.; Hofmeister, H.; Claus, P. *Catal. Today* **2002**, *72*, 63-78.
- (13) Haruta, M. *Catal. Today* **1997**, *36*, 153-156.

nm show very high activity in CO oxidation already at room temperature, despite the inertness of the bulk metal. Therefore, most attention is focused on oxidation reactions, and only very few new articles of other groups deal with the selective hydrogenation on gold catalysts.<sup>14–16</sup> This might be surprising, since the potential of supported gold catalysts for the selective hydrogenation of 1,3-butadiene has been evaluated by Bond et al. many years ago.<sup>17</sup>

Now our focus is directed on gaining more knowledge of how the unique behavior of gold is controlled by the nanostructure of the catalyst. Recently, we could show that activity and selectivity not only depended on particle size, but additional influences such as the degree of particle rounding or multiple twinning of gold particles had to be considered.<sup>1</sup> Therefore, one could hardly gain a deeper understanding of this process exclusively from particle size variations. In this work, we introduce quite another approach with a ZnO support enabling well-defined orientation relations of mainly single crystalline gold particles to influence the catalytic properties and to provide an easy morphology for the employment of a second metal applied by the addition of suitable amounts of indium. Usually the effect of a second metal is discussed in terms of modifications of existing active sites or creation of new ones.<sup>3–5</sup> We demonstrate that adding indium in an appropriate quantity just poisons undesired active sites, while the active sites, necessary to hydrogenate the C=O functional group in the presence of a C=C bond, remain unchanged. This allows us to control the hydrogenation properties of the active sites present on the gold particle surface.

## Experimental Section

Gold particles were deposited on ZnO (EGA Chemie, Germany) by a conventional impregnation procedure. An appropriate volume of the gold precursor HAuCl<sub>4</sub> was dissolved in water, and the resulting solution was brought into contact with the ZnO powder. This was followed by drying at 383 K for 2 h and subsequently reducing in a flow of hydrogen at 573 K for 3 h, resulting in a sample named Au/ZnO.

Additionally, indium was added to the reduced sample by impregnation with In(NO<sub>3</sub>)<sub>3</sub>·8H<sub>2</sub>O, corresponding to the pore volume of the support (“incipient wetness”), followed by drying at 293 K for 12 h and reducing a flow of hydrogen at 573 K for 2 h.

Characterization was performed mainly by conventional transmission electron microscopy (CTEM) on a JEM 1010 working at 100 kV as well as by high resolution transmission electron microscopy (HRTEM) on a JEM 4010 (400 kV). Energy-dispersive X-ray spectroscopy (EDX) was performed on a Philips CM 20 Twin working at 200 kV. For all TEM studies, the sample powder was dispersed in 2-propanol, agitated in an ultrasonic bath, and finally deposited on a commercial grade copper carrier grid (Grid 300, PLANO) which was coated with a carbon hole film. In the studies, preference was given to the areas near the holes. Subsequent image analysis was performed using Digital Micrograph (Gatan) and NIH Image software.<sup>18</sup>

The X-ray photoelectron spectra were obtained on a VG ESCALAB 220iXL spectrometer (VG Scientific) using monochromatized Al K $\alpha$

radiation (1486.6 eV) as the exciting source. Sample charging was reduced by use of a flood gun. For energy referencing, the peaks were corrected according to the Zn 2p<sub>3/2</sub> signal of ZnO with an assigned binding energy of 1022.3 eV.<sup>19</sup> The Auger parameter for In was quantified by the addition of the binding energy value of In 3d<sub>5/2</sub> and the kinetic energy of the InM<sub>4</sub>N<sub>45</sub>N<sub>45</sub> Auger electrons. All samples were treated in a hydrogen flux at 593 K for 2 h in a high-pressure gas cell installed in the lock to the analysis chamber, allowing a transfer to the spectrometer without air contact. The base pressure in the analysis chamber was 1 × 10<sup>-8</sup> Pa.

The metal content of a catalyst was estimated by atomic emission spectroscopy with inductively coupled plasma (OES-ICP, Perkin-Elmer Optima 3000XL) after dissolving the materials in a mixture of HF/HNO<sub>3</sub> by means of a MDS-2000 microwave unit (CEM).

The hydrogenation of acrolein (propenal, Aldrich) was realized in a computer controlled fixed-bed microreactor system described elsewhere.<sup>20</sup> Therewith, it is possible to carry out high-pressure gas phase hydrogenations of unsaturated organic compounds being liquids with low vapor pressure at standard conditions. In this study, we used the following standard test conditions: temperature 593 K, total pressure  $p_{\text{total}} = 2$  MPa, molar ratio hydrogen/acrolein  $\gamma = 20$ , reciprocal space time  $W/F_{\text{Ac},0} = 15.3$  g h mol<sup>-1</sup>, with  $W$  as the weight of the catalyst and  $F$  as the molar flow ratio. Deviations from these conditions are explicitly indicated in the text.

In principle, there are two possible reaction pathways. Adsorption, activation, and subsequent hydrogenation of the C=O group result in the production of allyl alcohol (propenol), which is the desired product. By hydrogenation of the C=C group in a parallel reaction, one obtains propionaldehyde (propanal), which can be produced principally also by isomerization of allyl alcohol. Furthermore, the production of *n*-propanol as a result of the subsequent reaction of allyl alcohol and/or propionaldehyde and C<sub>2</sub> and C<sub>3</sub> hydrocarbons (through decarbonylation, dehydration) is possible. For the temperature-programmed, online gas chromatographic separation of the reaction products and the nonconverted educt, a 30 m long DB capillary column was used.

The specific surface area and pore structure of the catalyst was characterized by nitrogen physisorption on a Sorptomatic 1990 (Fisons).

## Results

**Monometallic System Au/ZnO.** The BET surface of the ZnO support was 15 m<sup>2</sup>/g, as estimated by means of the physisorption of nitrogen. The mean diameter of the pores (45 nm) was calculated according to the method of Barrett, Joyner, and Halenda. Furthermore, no indications for the occurrence of micropores were found. ZnO particle sizes are in the range of about 100–500 nm, as evidenced by TEM (see also Figure 1). CTEM observations of the reduced sample revealed the occurrence of well separated crystalline gold particles in the nanometer size range (Figure 1). The particle size distribution derived from CTEM measurements fits well in a logarithmic normal distribution with a mean diameter  $d_{\text{Au}} = 9 \pm 0.3$  nm (Figure 2 (right)). By means of HRTEM, the crystal structure of individual gold particles was investigated, according to the method described recently.<sup>1</sup> Most particles were single crystalline (abbreviated as SC), whereas some of them showed planar defects (ST), as indicated in Figure 2 (right). Practically no multiply twinned particles (MTPs), as observed for other gold nanoparticle systems,<sup>1</sup> were found. Beside this, the gold particles are clearly well faceted (Figure 2 (left)), in contrast to those supported on other oxide supports such as ZrO<sub>2</sub> or TiO<sub>2</sub>.<sup>1</sup>

The particular structural characteristics of gold nanoparticles on a ZnO support are also reflected by the orientation relation-

(14) Jia, J.; Haraki, K.; Kondo, J. N.; Domen, K.; Tamaru, K. *J. Phys. Chem. B* **2000**, *104*, 11153–11156.

(15) Bailie, J. E.; Hutchings, G. J. *Chem. Commun.* **1999**, *21*, 2151–2152.

(16) Bailie, J. E.; Abdullah, H. A.; Anderson, J. A.; Rochester, C. H.; Richardson, N. V.; Hodge, N.; Zhang, J.-G.; Burrows, A.; Kiely, Ch. J.; Hutchings, G. J. *Phys. Chem. Chem. Phys.* **2001**, *3*, 4113–4125.

(17) (a) Bond, G. C.; Sermon, P. A.; Webb G.; Buchanan D. A.; Wells P. B. *J. Chem. Soc., Chem. Commun.* **1973**, 444–445. (b) Sermon, P. A.; Bond, G. C.; Wells, P. *J. Chem. Soc., Faraday Trans. 1* **1979**, *75*, 385–386.

(18) Rasband, W. NIH Image. Public domain software, U.S. National Institute of Health. <http://zippy.nimh.nih.gov>.

(19) NIST database for XP spectroscopy. <http://srdata.nist.gov/xps>.

(20) Lucas, M.; Claus, P. *Chem.-Ing.-Tech.* **1995**, *67*, 773–777.

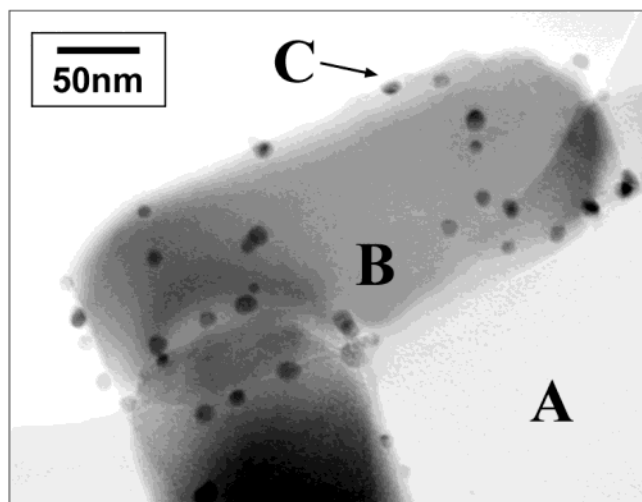


**Figure 1.** CTEM image of the freshly reduced sample Au/ZnO. The carbon film is indicated as A, the ZnO support as B, and the gold particles as C, respectively.

ships between the crystal lattice of the metal deposit and that of the oxide substrate, which were analyzed by HRTEM. The external shape of ZnO crystals, which exhibit the wurtzite lattice type, contains mainly (101), (100), (002), and (102) faces.<sup>21</sup> Quite according to the habit planes of ZnO, the grains of our model catalyst support are bounded by just these faces. On all these faces, in particular the most abundant (101) with {002}, {101}, and {102} lattice planes, an oriented growth of gold on ZnO was evidenced. Au{111} and Au{200} lattice planes were observed to be parallel to ZnO{101}. With respect to ZnO{100}, {002}, and {102} lattice planes, the orientation of Au{111} is slightly tilted by 3° to 8° out of the parallel alignment, accompanied by planar defects in numerous gold particles. This epitaxial growth behavior reduces the number of possible interface configurations considerably.

The results of the hydrogenation of acrolein are summarized in Table 1. Pure ZnO powder was proved to be completely unreactive (conversion < 0, 1%, i.e., below the detection limit).

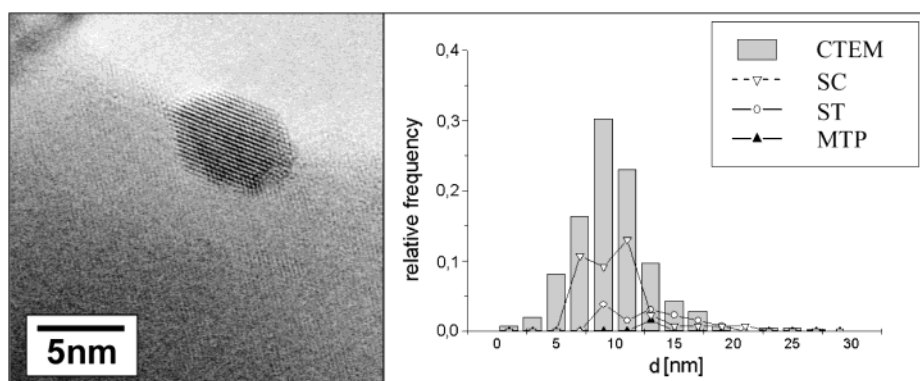


**Figure 2.** HRTEM image of the freshly reduced sample Au/ZnO (left); separate particle size distributions of the different occurring particle shapes together with particle size distribution derived from CTEM (right).

**Table 1.** Results of Catalytic Hydrogenation of Acrolein<sup>a</sup>

catalyst	$r$ [ $\mu\text{mol}/\text{g}_{\text{Au}} \text{sec}$ ]	AyOH	PA	<i>n</i> -PrOH	HC	$d_{\text{Au}}$ [nm]	<i>D</i>	TOF[1/s]
Au/ZnO	83.4	34.0	46.9	10.0	11.6	$9.0 \pm 0.3$	0.17	0.103
Au–In/ZnO	42.3	63.3	30.4	3.5	4.4	$10.1 \pm 0.2$	0.16	0.052

<sup>a</sup>Catalytic activities are expressed in terms of a rate related to the mass of the gold (abbreviated as *r*) as well as related to the surface area of gold (TOF). Possible products are allyl alcohol (abbreviated as AyOH), propionaldehyde (PA), *n*-propanol (*n*-PrOH), and C<sub>2</sub> and C<sub>3</sub> hydrocarbons (HC).

The sample Au/ZnO shows a selectivity to allyl alcohol of about 34%. Remarkable is, furthermore, a high selectivity to C<sub>2</sub>, C<sub>3</sub> hydrocarbons. This is not due to a dependence of selectivities on activity, since a variation of residence time did not induce significant changes in selectivities in the range of reciprocal space time  $W/F_{\text{Ac},0} = 7.4\text{--}15.3 \text{ g h mol}^{-1}$ .

The activity is given as the turnover frequency (TOF = 0.103 s<sup>-1</sup>), which has been estimated from the degree of dispersion. Together with a closed-shell particle model,<sup>22</sup> the latter is calculated from the mean gold particle diameter.

**Influence of Indium as Second Metal.** The reduced Au/ZnO sample was modified by the addition of an indium compound using the impregnation method as described previously. In the resulting sample Au–In/ZnO, the indium content was 0.13 wt % compared to 1.59 wt % for gold. This sample was characterized by applying different suitable methods. EDX investigations revealed a relatively homogeneous distribution of In on the Au particles (Figure 3). Besides, no monometallic indium deposits were found. By careful HRTEM image analysis, the lattice spacings of these bimetallic Au–In particles perpendicular to the outer surface were measured. Since there are distinct contrast differences between both metals, because of the atomic number difference, it was possible to distinguish for each atomic layer between both In and Au containing phases by this analysis. There is clear evidence of the formation of a separate indium phase, and only the first indium layer at the interface occasionally exhibits a kind of adaption to the lattice of the underlying metal (Figure 4).

The lattice distance of this indium phase measured by HRTEM is close to the (101) distance of tetragonal indium.

Furthermore, HRTEM imaging revealed clearly a selective deposition of indium on specific sites of the gold particle surface (Figure 5). Indium preferentially decorates the outer faces of the gold particles, while the edges remain uncovered. To support this observation, some statistical evaluation was undertaken (Table 2). Even though the number of particles analyzed is limited, there is clear evidence for this selective decoration.

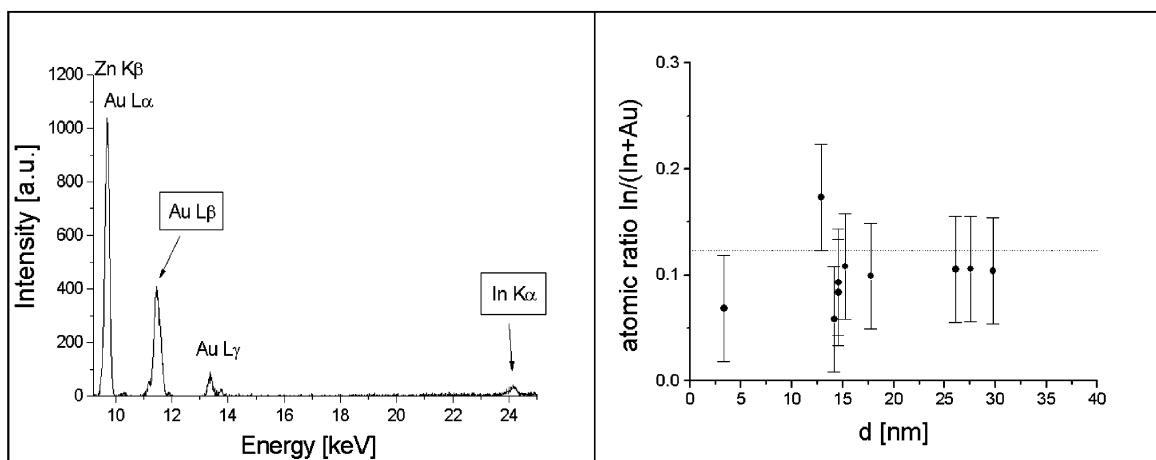


**Figure 3.** (Left) Typical EDX spectrum of a bimetallic Au–In particle of the sample Au–In/ZnO. (Right) Atomic ratio In/(In + Au) in dependence of bimetallic particle size. The dashed line indicates the corresponding macroscopic value, estimated via ICP–OES.

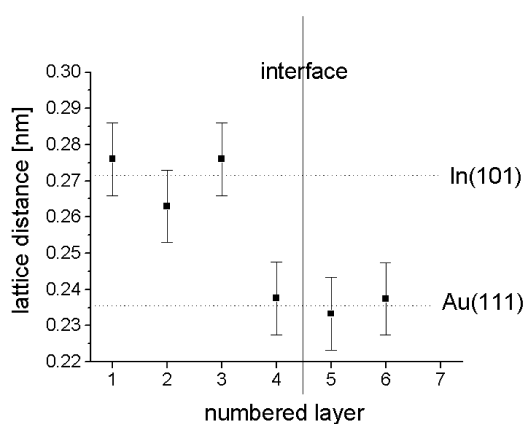


**Figure 4.** Evolution of lattice distances perpendicular to the surface within a bimetallic Au–In particle of the sample Au–In/ZnO, beginning from outer surface (numbered layer = 1), as derived from HRTEM image analysis. The horizontal dotted lines show the expected values for Au(111) and In(101) lattice distances. The vertical line indicates the interface between the two phases, identified by the difference of absorption contrast.

Besides a deposition of indium exclusively on the gold particles, at least a certain part of the interface Au–ZnO is also covered by indium.

The results of the hydrogenation of acrolein are summarized in Figure 6. When Au–In/ZnO is compared to Au/ZnO, there is a decrease in activity but a strong increase in selectivity to the desired allyl alcohol (from 36% to 63%). As a measure of yields, the site-time yields (STY) are used, which are the products of TOF and the respective selectivities. It is obvious that the addition of indium practically does not change the STY of allyl alcohol, while the STY of all other products are strongly depressed (Figure 7).

XP spectroscopy revealed an obvious influence of the treatment in hydrogen on the indium signal. Before a reduction in hydrogen, one In state with an In 3d<sub>5/2</sub> binding energy of 445.7 eV and an Auger parameter of 851.3 eV was found. After hydrogen treatment, the In 3d<sub>5/2</sub> peak reflects two electronic states for indium. The main component with a binding energy of 445.3 eV and an Auger parameter of 851.7 eV can be assigned to nonstoichiometric InO<sub>x</sub> ( $x < 1.5$ ).<sup>18</sup> Moreover, a

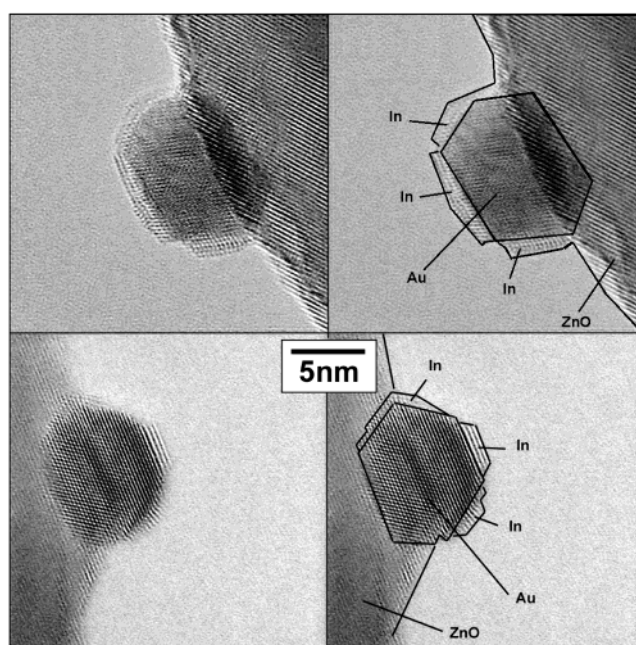


**Figure 5.** HRTEM images of Au–In/ZnO (left) plus same area with indicated structures (right).

**Table 2.** Statistics of Appearance of Indium on Specific Cuboctahedral Gold Surface Sites for Sample Au–In/ZnO

particles counted	completely without indium	only corners/edges free of In	only faces free of In	both faces and corners/edges free of In	in position not clear
67	2	31 ± 3	0	9 ± 3	24

second state with a binding energy of 444.1 eV was observed. Because of the small amount of this state, the kinetic energy of the Auger electrons could not be determined; however, the binding energy allowed a correlation with an oxidation state of zero for this In state.

**Modification of the Catalyst by the Reaction.** No significant difference in a mean particle size of about 9 nm was measured before and after reaction. However, electron microscopic observation of the spent sample revealed distinct changes of the gold particle configuration (Figure 7). The degree of faceting of the gold particles decreased during reaction. Remarkable is,

(21) Ertl, G.; Knözinger, H.; Weitkamp, J. *Handbook of Catalysis*; VCH: Weinheim, Germany, 1997; p 1525.

(22) Montejano-Carrizales, J. M.; Aguilera-Granja, F.; Moran-Lopez, J. L. *Nanostruct. Mater.* **1997**, *8*, 269–287.

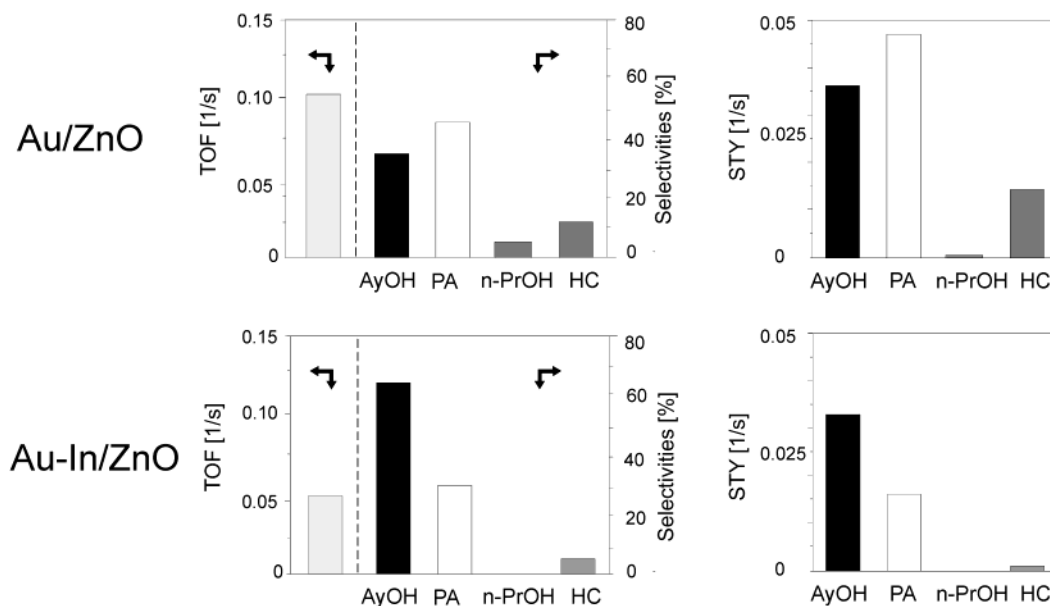


**Figure 6.** Results of catalytic tests in hydrogenation of acrolein at 593 K. The yields are expressed in terms of the site-time yield (STY), which is the product of TOF and the respective selectivity. Possible products are allyl alcohol (propenol, abbreviated as AyOH), propionaldehyde (propanal, PA), *n*-propanol (*n*-PrOH), and C<sub>2</sub> and C<sub>3</sub> hydrocarbons (HC).

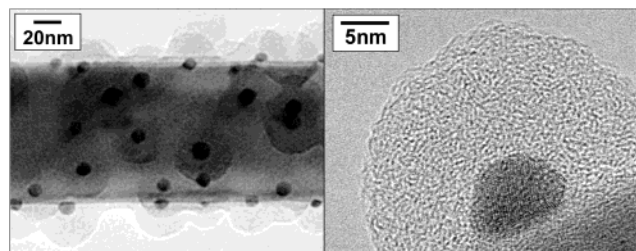


**Figure 7.** Amorphous shells around gold particles for spent sample Au/ZnO: CTEM image (left) and HRTEM image (right).

furthermore, the occurrence of pronounced amorphous shells around almost all gold particles and gold–indium particles, respectively, which were not observed in analogous gold catalysts on other supports.<sup>11,12,23</sup> Analysis of EDX spectra revealed that these shells consisted of carbon or a carbon-containing material. Thus, they are most probably remnants of reaction products still sticking on the gold surface.

Even though the contrast of indium layers on small gold particles in the spent sample is superimposed by the contrast of the carbonaceous shell, making a quantitative analysis much more complicated, at least for larger particles the preferred decoration of gold faces by indium, still being present, could be verified.

## Discussion

Usually, an ideal cuboctahedral particle shape is assumed to model the structure sensitivity of the hydrogenation of  $\alpha,\beta$ -unsaturated aldehydes catalyzed by supported metal particles.<sup>6,7</sup> Indeed, this is the equilibrium shape for face centered cubic crystals at 0 K, as it results from thermodynamical considerations via the so-called Wulff plot.<sup>25</sup> In a certain size range, the relative portion of atoms situated in (111) surfaces of

cuboctahedra increases with size. Therefore, the increase of selectivity to the unsaturated aldehyde with the increasing size of metal particles was explained by (111) faces containing the active sites for the adsorption and subsequent hydrogenation of the C=O group.<sup>5,9,23,24</sup> However, under reaction conditions the metal particles on the oxide support are rounded to a certain extent and partly exhibit a multiply twinned structure. The effect of these deviations from the previous model may hamper the explanation of structure sensitivity simply based on particle size dependent changes of the amount of various surface sites (atoms in corners, edges, or faces, etc.). We could show, recently, that a high number of multiply twinned gold particles decreases both TOF and selectivity to allyl alcohol.<sup>1</sup> Moreover, the higher TOF on Au/TiO<sub>2</sub> compared to Au/ZrO<sub>2</sub> was attributed to the larger extent of rounded particles of the titania catalyst.<sup>1</sup> A variation of the particle size, of course, influences all factors governing the reactivity, and therefore, no specific statements on the nature of active sites are possible. Furthermore, a certain influence of the configuration of the metal particle–oxide support interface in this process cannot be excluded.

Even though metal particles on powder supports used in catalysis may exhibit a certain degree of oriented overgrowth, it usually plays only a minor role, since such supports are characterized by a high specific surface area, the occurrence of pores in the nanometer range, a vast number of grain boundaries, and many different crystal faces. One exception is the epitaxial orientation of Pt and Ni islands of 1 monolayer height on various faces of  $\gamma$ -Al<sub>2</sub>O<sub>3</sub> powder.<sup>21</sup> An even more important example concerns the use of ZnO supports. Metha et al. reported on preferred epitaxial relationships between copper particles and the support in Cu/ZnO catalysts applied for methanol synthesis.<sup>22</sup> The ZnO used in this study is unique because of its low specific surface, the absence of nanometer-sized pores, and extended defect-free surface areas. Furthermore, the lattice spacings of the metal and support allow orientation relations of low lateral misfit, favoring the previously reported epitaxial growth behavior. Simultaneously, the extent of rounded gold particles is

(23) Mohr, C.; Hofmeister, H.; Lucas, M.; Claus, P. *Chem. Eng. Technol.* **2000**, *3* (4), 324–328.

(24) Coq, B.; Choune, A.; Nciri, B. *Appl. Catal. A: General* **1992**, *82*, 231–245.

(25) Henry, C. R. *Surf. Sci. Rep.* **1998**, *31*, 235.

smaller for Au/ZnO than for Au/TiO<sub>2</sub> or Au/ZrO<sub>2</sub>,<sup>1</sup> and the occurrence of multiply twinned particles is strongly suppressed. Consequently, this Au/ZnO system matches the requirements for a well-defined model catalyst. The almost exclusive occurrence of single crystalline gold particles with pronounced faceting after a reduction in hydrogen allows application of a cuboctahedron model<sup>28</sup> for gold particles of that special catalyst. This results in a limited number of types of possible active sites.

The ZnO support itself is unreactive. Since ZnO is not reducible by flowing hydrogen up to 673 K,<sup>29</sup> an electronic interaction between ZnO and Au during this reduction process is improbable. Furthermore, for a mean gold particle size of about 9 nm, atoms in corners may be neglected as well as any quantum size related effects. Therewith, the catalytic behavior may be interpreted as a competition between active sites on edges, on faces, and at the interface gold–support.

With this well-defined catalyst, a new approach, namely the addition of indium as second metal, was introduced. According to Coq et al.,<sup>24</sup> the characterization of such a bimetallic system has to answer three questions: (i) Are there unexceptionally bimetallic particles? (ii) If yes, are there segregations of one component on the surface? (iii) If yes, are there preferred places of deposition of that component? All of these questions could be answered in a satisfactory way. By EDX spectroscopy, it has been shown that only bimetallic Au–In particles occur. The In/Au ratio changes only slightly between different particles. The segregation of indium on the surface of the gold particles was evidenced by measurement of the evolution of lattice distances perpendicular to the surface of the bimetallic particles. Even though the measurement of the lattice distance points to the occurrence of tetragonal indium, XPS measurements strongly suggest the (additional) occurrence of indium suboxides (InO<sub>x</sub>,  $x < 1$ , 5) under the same conditions, which probably exhibits similar lattice distances. From theoretical considerations, one might have expected the occurrence of Hume–Rothery phases or intermetallic phases.<sup>30</sup> For indium amounts below about 10 wt %, as it is the case for the sample discussed here, the hexagonal phases  $\alpha_1$  ( $a = 0.290\ 90$  nm,  $c = 0.95\ 000$  nm) and  $\zeta$  ( $a = 0.28\ 995$  nm,  $c = 0.47\ 801$  nm) are stable. However, the existence of these phases can be clearly ruled out by comparison of the respective lattice distances. With that, the occurrence of mixed-crystal phases should be excluded. A possible partial oxidation of indium does not influence the following interpretation.

A more detailed analysis revealed clearly that the indium-containing phase decorates preferentially the faces of the gold particles and at least partially the interface gold–support, while the edges of the cuboctahedral gold particles remain uncovered. The content of indium corresponds to a nominal mean coverage of indium on the surface of the gold particles of about 0.9 monolayers, by the simplifying assumption of unsupported cuboctahedral gold particles and adaption of the crystal structure of gold by indium. A more accurate estimation should include that a certain part of the gold surface is in direct contact to the ZnO support. If one assumes that half of the surface of the gold

particles is in direct contact with the ZnO support, this shifts the “real” mean coverage of indium to a value of roughly 2 monolayers. Furthermore, from a visual observation of Figure 5, it is obvious that the degree of coverage of the first layer of indium is higher than that of the second one, which itself is higher than that of the third, and so forth. Keeping all this in mind, we find the rough estimation of the “real” degree of coverage is in relative good agreement with the HRTEM images in Figure 5.

The observation of the selective decoration of the faces of the gold particles by indium is in total contradiction to all assumptions and observation made before. The surface energy of indium (0.6 J/m<sup>2</sup>) is significantly lower than that of gold (1.2 J/m<sup>2</sup>).<sup>31</sup> Up to now, a decoration with a second metal having a lower surface energy has been thought to occur preferentially on low-coordinated surface sites, that is, corners and edges. This was also supported by Monte Carlo simulations for the deposition of Cu, Ag, Au on perfect Pt cuboctahedra,<sup>32</sup> or Sn on Rh particles.<sup>33</sup>

The only reasonable explanation of the observed effect is due to the interaction of the gold surface with hydrogen. It is well-known that gold surfaces do not interact substantially with hydrogen,<sup>16</sup> while this might be different for low-coordinated gold surface sites (i.e., edges). Indeed, it has been demonstrated that the binding energy of CO on the (111) facets of Pd clusters is lowered compared to that on edges or even corners.<sup>25</sup> This could decrease the value of the configuration energy of edges (corners) below the value of the faces, making an indium segregation on the faces thermodynamically preferable. For example, it has been calculated that the interaction of hydrogen with (100), (111), and (110) surfaces of diamond and silicon should change the surface anisotropy.<sup>34</sup> Moreover, Khanra and Menon used Monte Carlo simulations to study the interaction of CO with Pd–Cu bimetallic clusters. While for clean particles of all sizes the surface is enriched in Cu, with an increase in CO adsorption the extent in Cu segregation gradually reduces, leading to a Pd segregation at higher CO coverage.<sup>35</sup>

The selective decoration of gold faces by indium is accompanied by a decrease in activity and a strong increase in selectivity to the desired allyl alcohol. The yield of allyl alcohol remains constant, while the yields of all other products decrease. A direct influence of indium may be neglected, since the activity as well as selectivity to allyl alcohol on monometallic indium catalysts is much lower compared to gold.<sup>36</sup> In a generalized context of possible influences of a second metal on the behavior of supported metal catalysts in the hydrogenation of  $\alpha,\beta$ -unsaturated aldehydes, an increase of the selectivity to unsaturated alcohols may be due to either an electronic modification of the active sites or a selective decoration of those active sites producing preferentially the undesired products.<sup>3–5,37</sup> An electronic modification can be expected to be accompanied by structural rearrangements, in particular by the occurrence of mixed crystal phases. Since such behavior was not observed,

(26) Stakheev, A. Y.; Kustov, L. M. *Appl. Catal. A: General* **1999**, *188*, 3–35.  
(27) Mehta, S.; Simmons, G. W.; Klier, K.; Herman, R. G. *J. Catal.* **1979**, *57*, 339–360.  
(28) van Harfeld, R.; Hartog, F. *Surf. Sci.* **1969**, *15* (2), 189–230.  
(29) Jung, K. D.; Joo, O. S.; Han, S. H. *Catal. Lett.* **2000**, *68* (1–2), 49–54.  
(30) New series IV/5; Landolt–Börnstein.

(31) Chang, Z. C.; Lu, F. H.; Shieu, F. S. *Mater. Chem. Phys.* **2001**, *70*, 137–143.  
(32) Coq, B.; Choune, A.; Goursot, A.; Tazi, T.; Figueras, F.; Salahu, D. R. *J. Am. Chem. Soc.* **1991**, *113*, 1485–1492.  
(33) Strohl, J. K.; King, T. S. *J. Catal.* **1989**, *116*, 540–555.  
(34) Hong, S.; Chou, M. Y. *Phys. Rev. B* **1998**, *11* (57), 6262–6265.  
(35) Khandra, B. C.; Menon, M. *Int. J. Mod. Phys. B* **1999**, *13*(1), 59–71.  
(36) Mohr, C.; Claus, P. *Sci. Prog.* **2001**, *84* (4), 311–334.  
(37) Bond, G. *Chem. Soc. Rev.* **1991**, *20*, 441–475.

the only explanation of the experimental observations is the selective decoration of undesired active sites. Thus, it becomes clear that the hydrogenation of the C=O group, that is, the production of allyl alcohol, works best on the edges of cuboctahedral gold particles. The faces of gold particles, on the other hand, should favor the formation of the undesired products. High yields of C<sub>2</sub>, C<sub>3</sub> hydrocarbons point to the role of the unique Au–ZnO interface resulting from epitaxial growth, since such yields are not observed for gold catalysts on other supports.<sup>11,12,23</sup> Even though the latter could not be proved directly, it is clear that the interface Au/ZnO does not provide active sites for the hydrogenation of the C=O group, as supposed by Bailie and Hutchings.<sup>15</sup>

It is not fully excluded that during the preparation Zn<sup>2+</sup> ions are diluted out of the ZnO support surface. These ions might be (partially) reduced during hydrogen treatment which could lead to Au–Zn alloy formation. However, no evidence for a deposition of Zn on the surface of gold particles was found whether by HRTEM or by EDX. It should be mentioned that Au/ZnO catalysts used by Bailie et al. for the selective hydrogenation of croton aldehyde were basically prepared in the same way.<sup>16</sup>

The observed behavior also agrees with IR spectroscopy results of acrolein.<sup>38</sup> The intensity ratio of C=O stretching vibrations to corresponding C=C stretching vibrations was distinctly enhanced on polycrystalline films with a high content of crystal edges between various corners compared to extended single-crystal Au(111) surfaces. Even though it is not clear whether our assignment of active sites can be transferred to the

properties of other catalytic systems, it is remarkable that these findings are in a few important points in clear contradiction to earlier assumptions.

## Conclusions

By the addition of a second metal, namely indium, to a well-defined catalyst, consisting of well faceted and oriented gold nanoparticles on ZnO powder support, we introduced a new approach to the study of active sites in the hydrogenation of  $\alpha,\beta$ -unsaturated aldehydes. For the first time, it has been demonstrated that the addition of a second metal (indium) can result in a selective decoration of the faces of gold particles. This has some important implications for the selective hydrogenation of acrolein on gold chosen as a test reaction. Even though (111) and (100) faces of gold nanoparticles are active in hydrogenation, they produce preferentially propionaldehyde. On edges (and maybe also on corners), allyl alcohol is mainly produced, with maximum selectivities above 60%. It has been shown that the desired activation of the C=O group in the selective hydrogenation of acrolein is not related to the gold–support interface. An increasing amount of C<sub>2</sub>, C<sub>3</sub> hydrocarbons is attributed to the occurrence of a unique interface, owing to the epitaxial growth behavior of Au on ZnO.

**Acknowledgment.** This work has been supported by the Federal Ministry for Science and Education under Grant 03D0028A0. P.C. thanks the Fonds der Chemischen Industrie for financial support. C.M. thanks Dr. U. Richter from Labor für Elektronenmikroskopie, Halle and Dr. H. Stenzel from MPI of Microstructure Physics, Halle for cooperation in EDX spectroscopy.

(38) Akita, M.; Osaka, N.; Itoh, K. *Surf. Sci.* **1998**, *405* (2–3), 172–181.